

Turbulent spectra and spectral kinks in the transition range from MHD to kinetic Alfvén turbulence

Y. Voitenko and J. De Keyser

Belgian Institute for Space Aeronomy, Brussels, Belgium

Abstract. A weakly dispersive sub-range (WDR) of kinetic Alfvén turbulence is distinguished and investigated for the first time in the context of MHD/kinetic turbulence transition. We found perpendicular wavenumber spectra $\propto k_{\perp}^{-3}$ and $\propto k_{\perp}^{-4}$ formed in WDR by strong and weak turbulence of kinetic Alfvén waves (KAWs), respectively. These steep WDR spectra connect shallower spectra in the MHD and strongly dispersive KAW sub-ranges, which results in a specific double-kink (2-k) pattern often seen in observed turbulent spectra. The first kink occurs where MHD turbulence transforms into weakly dispersive KAW turbulence; the second one is between weakly and strongly dispersive KAW sub-ranges. Our analysis suggests that the partial turbulence dissipation due to amplitude-dependent super-adiabatic ion heating may occur in the vicinity of the first spectral kink. A threshold-like nature of this process results in a conditional selective dissipation affecting only largest over-threshold amplitudes and decreasing intermittency in the range below the first spectral kink. Several recent counter-intuitive observational findings can be explained by the selective dissipation coupled to the nonlinear interaction among weakly dispersive KAWs.

1 Introduction

Kinetic Alfvén waves (KAWs) are an extension of MHD Alfvén waves in the range of high perpendicular wavenumbers k_{\perp} in the plane $\perp \mathbf{B}_0$, where linear and nonlinear effects due to finite values of $\mu = k_{\perp} \rho_i$ become significant ($\mathbf{B}_0 \parallel z$ is the background magnetic field, $\rho_i = V_{Ti}/\Omega_i$ is the ion gyro-radius) (Hasegawa and Chen, 1976; Voitenko, 1998a). There are numerous observational and theoretical indications that MHD Alfvén turbulence in the solar wind cascades towards

high k_{\perp} and eventually reaches the KAW wavenumber range at the proton gyroradius scales, $k_{\perp} \rho_p \sim 1$ (Leamon et al., 1999; Bale et al., 2005; Alexandrova et al., 2008; Sahraoui et al., 2010). It is not yet certain what happens next with these KAWs: do they dissipate heating plasma (Leamon et al. 1999), or interact nonlinearly among themselves and proceed cascading further towards higher k_{\perp} , reaching electron scales (Alexandrova et al., 2008; Sahraoui et al., 2010). It has been envisaged that the nonlinear evolution and related wavenumber spectra in the range below the spectral break point $k_{\perp b} \sim \rho_p^{-1}$ are dominated by MHD-type nonlinear interactions among Alfvén waves, and the spectra at $k_{\perp} > k_{\perp b}$ are determined by linear and nonlinear properties of KAWs. If the dissipation is more efficient, the cascade should dissipate in the vicinity of $k_{\perp b}$ and cannot reach electron scales, as was argued by Leamon et al. (1999), Howes et al. (2008), and Podesta et al. (2009) using Landau damping estimations. There are, however, observational indications (see Sahraoui et al., 2010, and references therein), that the nonlinear interaction among KAWs is faster than their dissipation, and the turbulence cascade proceeds further at higher $k_{\perp} \rho_p \gg 1$ creating a kinetic-scale turbulence of KAWs.

From observational point of view, the transformation occurs at the spectral break points f_b dividing shallower MHD spectra $\propto f^{-5/3}$ at $f < f_b$ and steeper kinetic spectra with power indexes ranging from -2 to -4 at $f > f_b$, which are observed in the solar wind (f is the frequency in the satellite frame). Because of the large solar wind velocity, $V_{SW} \gg V_A$, the Alfvénic time variations $\omega_A \sim k_z V_A$ are usually much slower than the Doppler frequencies in satellite frame $\omega_d = \mathbf{k} \cdot \mathbf{V}_{SW}$ (Taylor hypothesis). Then the satellite-frame frequency spectra are dominated by the Doppler frequency, $2\pi f = |k_z V_A - \mathbf{k} \cdot \mathbf{V}_{SW}| \sim |\mathbf{k} \cdot \mathbf{V}_{SW}|$, representing wave-number spectra. As the solar wind turbulence is dominated by large perpendicular wave vectors $k_{\perp} \gg k_z$ (Sahraoui et al., 2010; Luo and Wu, 2010, and references therein), satellites measure perpendicular wavenumber spec-

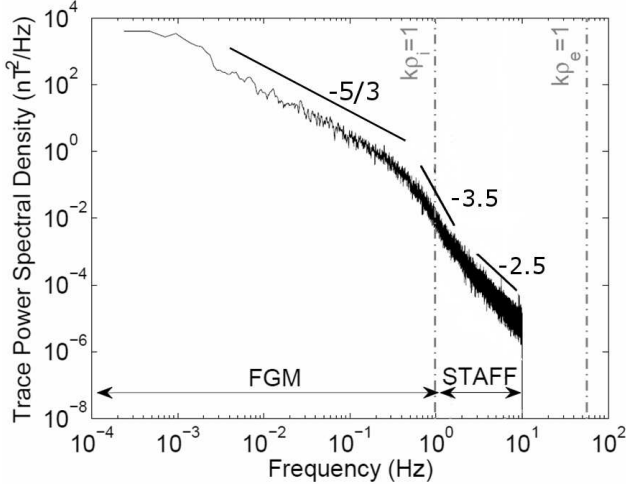


Fig. 1. Turbulent Alfvénic spectrum extending over three sub-ranges, with the steepest slope in the weakly/mildly dispersive KAW sub-range (interpretation of the spectrum shown in Fig. 1 by Chen et al., 2010)

tra, $f \propto k_{\perp}$. There are of course rare cases $\mathbf{B}_0 \parallel \mathbf{V}_{SW}$, where frequency measures parallel wavenumber, $f \propto k_z$. The spectral break f_b of the turbulence is often associated with one of the proton kinetic scales, proton gyroradius ρ_p or proton inertial length $\delta_p = V_A/\Omega_i$, such that the observed break-point frequency $2\pi f_b \simeq V_{SW}/\rho_p$ or V_{SW}/δ_p (Leamon et al., 1999; Bale et al., 2005; Alexandrova et al., 2008; Sahraoui et al., 2010).

Because of the complex interplay between linear and non-linear dynamics of KAWs, theoretical interpretation of the turbulence, its dissipation, and related spectra in the KAW range is still incomplete. In particular, recent theoretical analysis by Podesta et al. (2010) argues that the KAW cascade subject to collisionless Landau damping cannot reach electron scales in the solar wind conditions, which contradicts the opposite conclusion by Sahraoui et al. (2010) based on observations. Using Cluster data, Sahraoui et al. (2010) found that the wavenumber spectra of MHD and KAW turbulences have slopes $\propto k_{\perp}^{-1.7}$ and $\propto k_{\perp}^{-2.8}$, respectively, and the KAW turbulence extends to electron scales in the solar wind at 1 AU (Sahraoui et al., 2010). Between these $k_{\perp}^{-1.7}$ and $k_{\perp}^{-2.8}$ spectra, Sahraoui et al. (2010) also noticed much steeper $\propto k_{\perp}^{-4}$ spectra that appear in the weakly/mildly dispersive KAW sub-range $0.6 < k_{\perp}\rho_p < 2$ (see their Fig. 1). The same spectral form in the MHD/kinetic transition range, containing two spectral kinks with steepest spectra inbetween, can be seen in other recent studies - see example in Fig.1 adopted from the paper by Chen et al. (2010) (see also Fig. 1 by Smith et al., 2006).

Steep variable spectra in the same wavenumber range were observed before (Leamon et al. 1999), but without connection to shallower higher-wavenumber (higher-frequency in

the satellite frame) spectra that were unavailable. These steep spectra were called the "dissipation range" spectra, and were associated with dissipation, mainly via kinetic ion-cyclotron and Landau damping. However, the nature of the "dissipation range" and its spectra is not so clear. For example, recent observations of reduced magnetic helicity imply the presence of counter-streaming KAWs surviving the "dissipation range" rather than ion-cyclotron damping in it (Carbone et al. 2010).

Analyzing ACE spacecraft data, Smith et al. (2006) have found that the larger spectral fluxes (as measured at 0.01 Hz) are followed by the steeper spectra in the "dissipation range" above the spectral break $f_b \sim 0.3$ Hz. This counterintuitive observational fact is difficult to explain by ion-cyclotron and Landau damping. Smith et al. (2006) did not find any regular dependence of f_b on the cascade rate. However, later on Markovskii, Vasquez, and Smith (2008) studied the statistics and scaling of the spectral breaks and concluded that their positions are determined by a combination of their scales and the turbulent amplitudes at that scales, which suggests a non-linear dissipation mechanism for the solar wind turbulence. Again, kinetic ion-cyclotron and Landau damping mechanisms would not lead to such behavior of the dissipation range.

Motivated by these findings, in the present paper we analyze the transition wavenumber range from MHD to KAW turbulence focusing on nonlinear KAW properties. We demonstrate that the observed spectral forms and steep spectra in the "dissipation range" can be explained by the nonlinear interaction of weakly dispersive KAWs without involving kinetic ion-cyclotron and Landau dissipation mechanisms.

2 Weakly dispersive $k_{\perp}\rho_p < 1$ sub-range of the KAW turbulence

In the weakly dispersive range, in the limit $k_{\perp}^2\rho_p^2 \ll 1$, the rate of the nonlinear interaction among highly oblique $k_z \ll k_{\perp}$ co-propagating KAWs is calculated by maximizing the matrix element of the 3-wave KAW interaction calculated by Voitenko (1998a,b):

$$\gamma_{k\uparrow\uparrow}^{NL} \simeq 0.4\Omega_p \frac{V_A}{V_{Tp}} \mu^3 \frac{B_k}{B_0}, \quad (1)$$

where B_k is the KAW amplitude at the (anisotropic) length scales $\lambda_z = 2\pi/k_z$; $\lambda_{\perp} = 2\pi/k_{\perp}$, where k_z and k_{\perp} are parallel and perpendicular KAW wavenumbers. We put $T_{e\parallel}/T_{p\perp} = 1$ in (1) and further on for simplicity.

In the KAW case $k_{\perp} \gg k_z$ and the nonlinear wave dynamics is driven by the energy exchange among short cross-field length scales, whereas the parallel scales follow the perpendicular ones kinematically (in the weak turbulence) or via critical balance (in the strong turbulence). Then the amplitude B_k can be related to the omnidirectional spectral energy density $W_{k\perp}$ as $B_k = \sqrt{k_{\perp} W_{k\perp}}$ ($W_{k\perp}$ is defined such that $\int_0^{\infty} dk_{\perp} W_{k\perp} = \text{total fluctuation energy per unit volume}$).

The nonlinear interaction rate of counter-propagating $\mu \ll 1$ KAWs is (Voitenko, 1998a,b)

$$\gamma_{k\uparrow\downarrow}^{NL} \simeq 0.3\Omega_i \frac{V_A}{V_{Ti}} \mu^2 \frac{B_k}{B_0}. \quad (2)$$

In the weakly dispersive sub-range $\gamma_{k\uparrow\uparrow}^{NL} < \gamma_{k\uparrow\downarrow}^{NL}$, but short linear correlation time among counter-propagating KAWs can reduce the counter-propagating nonlinear rate below $\gamma_{k\uparrow\uparrow}^{NL}$. Note that there is no explicit k_z -dependence in the above expressions for interaction rates.

2.1 Weak KAW turbulence

The nonlinear interaction among co-propagating KAWs can be considered weak if their nonlinear rate (1) is less than the dispersive part of the KAW frequency: $\gamma_k^{NL} < \delta\omega_k$, where $\delta\omega_k \simeq k_z V_A \mu^2$ in isothermal plasmas. In this case, the conservation law for the generalized enstrophy (dispersive part of energy) apply, and nonlinear interaction among co-propagating KAWs (1) establishes perpendicular wavenumber spectra

$$W_k \propto k_\perp^{-5}; \quad (3)$$

$$W_k \propto k_\perp^{-4}, \quad (4)$$

created by the direct enstrophy and inverse energy cascades, respectively (Voitenko, 1998b).

For the axially symmetric turbulence in the cross-field plane we can define a reduced omnidirectional spectral power $W_{k\perp} = 2\pi k_\perp \int dk_z B_k^2$, such that $W = \int dk_\perp W_{k\perp}$. The energy exchange among different k_\perp does not depend on k_z (cf. eqs (6.1) and (6.2) by Voitenko (1998a)). Hence the weakly turbulent 3D spectra (3-4) have their corresponding reduced omnidirectional power spectra

$$W_{k\perp} \propto k_\perp^{-4}, \quad (5)$$

$$W_{k\perp} \propto k_\perp^{-3}. \quad (6)$$

The omnidirectional wavenumber spectra are those measured in the solar wind by satellites as 1D Doppler frequency spectra if the solar wind velocity $\mathbf{V}_{SW} \nparallel \mathbf{B}_0$. In the case of turbulent spectra that are axially asymmetric around B_0 axis, the measured 1D spectrum may have a larger power index, approaching $W_{k\perp} \propto k_\perp^{-5}$ in the extreme case of flat turbulence (say, $\propto k_x^{-5}$). Accounting for a possible anisotropy, the steepest spectra produced by the weakly dispersive turbulence are

$$W_{k\perp} \propto k_\perp^{-4} \div k_\perp^{-4.5}. \quad (7)$$

Nonlinear interaction among counter-propagating KAWs (2) produces an imbalanced turbulence with weakly turbulent omnidirectional spectra

$$W_{k\perp} \propto k_\perp^{-2}; \quad (8)$$

$$W_{k\perp} \propto k_\perp^{-1}, \quad (9)$$

created by the direct enstrophy and inverse energy cascades, respectively (Voitenko, 1998b). The counter-propagating interactions cannot produce steep observed spectra in the transition range.

At first sight, interaction among counter-propagating KAWs in the weakly dispersive range is stronger than among co-propagating KAWs: $\gamma_{k\uparrow\downarrow}^{NL} \gg \gamma_{k\uparrow\uparrow}^{NL}$ for $\mu \ll 1$. However, short correlation times among counter-propagating KAWs, $\tau_{c\uparrow\downarrow} \sim \lambda_z/V_A$, can reduce their interaction strength as compared to the co-propagating KAWs that keep in phase longer time, $\tau_{c\uparrow\uparrow} \sim \mu^{-2}\lambda_z/V_A \gg \tau_{c\uparrow\downarrow}$ for $\mu \ll 1$. In this case, the dominant (outward-propagating in the solar wind) component of the imbalanced turbulence will be shaped by the nonlinear interaction among co-propagating KAWs with omnidirectional spectra (7), as described above.

The k_z spectra of the weak KAW turbulence are determined by the kinematics of three-wave resonant interactions:

$$W_{k\parallel} \propto k_z^{-1/2}. \quad (10)$$

However, some non-kinematic factors, like finite resonance width, can make the parallel spectrum significantly different from (10). This point needs further investigation.

2.2 Strong KAW turbulence

In the strongly turbulent regime the nonlinear time scale $\tau_k^{NL} (\sim 1/\gamma_k^{NL})$ becomes equal to or larger than the linear one, $\tau_k^L (\sim 1/\delta\omega_k)$, so that the enstrophy should not be conserved any more. In this regime we find the energy k_\perp -spectrum from the condition that the energy flow through any k_\perp does not depend on k_\perp :

$$\varepsilon \sim B_k^2/\tau_k^{NL} = \text{const}. \quad (11)$$

The nonlinear evolution time for co-propagating KAWs can be estimated as $\tau_{k\uparrow\uparrow}^{NL} \simeq 1/\gamma_{k\uparrow\uparrow}^{NL}$, where $\gamma_{k\uparrow\uparrow}^{NL}$ is given by (1).

Then from (11) we find the scaling for the fluctuating magnetic amplitude $B_k \propto k_\perp^{-1}$, which results in the omnidirectional energy spectrum

$$W_{k\perp} \sim \frac{B_k^2}{k_\perp} \propto k_\perp^{-3}. \quad (12)$$

Again, one can observe steeper spectra $\propto (k_\perp^{-3} \div k_\perp^{-4})$ if the strong KAW turbulence is not exactly axially symmetric around B_0 .

Since $\gamma_{k\uparrow\uparrow}^{NL}$ depends on k_z only through B_k , the k_z -dependence can appear via any functional form with argument involving some combination of k_z and k_\perp . Additional assumptions linking k_z and k_\perp , like critical balance hypothesis, will be studied in another paper.

The strongly turbulent spectra of weakly dispersive counter-propagating KAWs can be found from (11) with $1/\tau_k^{NL} \sim \gamma_{k\uparrow\downarrow}^{NL}$ given by (2):

$$W_{k\perp} \sim \frac{B_k^2}{k_\perp} \propto k_\perp^{-7/3} \quad (13)$$

3 Strongly dispersive $k_\perp \rho_p > 1$ sub-range of the KAW turbulence

In the strongly dispersive sub-range of KAWs $\mu > 1$, which was considered in the literature and named as the "KAW range" (see Schekochihin et al., 2009, and references therein), the rate of nonlinear interaction among co-propagating KAWs is (Voitenko, 1998a;b)

$$\gamma_{k\uparrow\uparrow}^{NL} \simeq 0.3\Omega_i \frac{V_A}{V_{Ti}} \mu^2 \frac{B_k}{B_0}. \quad (14)$$

For counter-propagating KAWs, the nonlinear interaction rate is almost the same,

$$\gamma_{k\uparrow\downarrow}^{NL} \simeq 0.2\Omega_i \frac{V_A}{V_{Ti}} \mu^2 \frac{B_k}{B_0}.$$

3.1 Weak turbulence ($\gamma_k^{NL} \ll \omega_k$)

The weakly turbulent perpendicular wavenumber spectra of co-propagating KAWs,

$$B_k^2 \propto k_\perp^{-7/2}; \quad (15)$$

$$B_k^2 \propto k_\perp^{-3},$$

are created by the direct energy and inverse enstrophy cascades, respectively (Voitenko, 1998b). Again, the nonlinear rate for the counter-propagating KAWs can be reduced by shorter linear correlation times as compared to the co-propagating KAWs. Therefore, the omnidirectional spectra

$$W_{k\perp} \propto k_\perp^{-5/2}, \quad (16)$$

$$W_{k\perp} \propto k_\perp^{-2} \quad (17)$$

can be formed by strongly dispersive KAWs in the weakly turbulent regime. Among these, the $\propto k_\perp^{-5/2}$ spectrum formed by the direct energy cascade is preferable. With local deviations from axially symmetry, one can expect steeper spectra $\propto k_\perp^{-2.5} \div k_\perp^{-3}$.

3.2 Strong turbulence ($\omega_k \sim \gamma_k^{NL}$)

In the strong turbulence of co-propagating KAWs, the scaling of magnetic field amplitude B_k with k_\perp is found from the condition (11) where $\tau_k^{NL} \simeq 1/\gamma_{k\uparrow\uparrow}^{NL}$ with $\gamma_{k\uparrow\uparrow}^{NL}$ given by (14):

$$B_k \propto k_\perp^{-2/3}.$$

This results in the familiar omnidirectional energy spectrum in k_\perp :

$$W_{k\perp} \sim \frac{B_k^2}{k_\perp} \propto k_\perp^{-7/3}. \quad (18)$$

The "parallel" $k_z \parallel B_0$ spectrum

$$W_{k\parallel} \propto k_z^{-2} \quad (19)$$

follows from the critical balance condition.

4 MHD/kinetic Alfvén transition

4.1 Spectral kinks

In the Goldreich and Sridhar (1995) MHD model, the AW nonlinear interaction rate at scale λ_\perp in the plane $\perp B_0$ can be written as

$$\gamma_k^{GS} \simeq \frac{v_{\lambda\perp}}{\lambda_\perp} \simeq \frac{1}{2\pi} k_\perp V_A \frac{B_k}{B_0}, \quad (20)$$

where $v_{\lambda\perp}$ is the velocity and B_k is the magnetic field amplitude at the scale $\lambda_\perp = 2\pi/k_\perp$. The corresponding MHD AW spectrum $B_k^2 \propto k_\perp^{-2/3}$ follows from the independence of the energy flux through k . The omnidirectional spectrum $W_k \sim B_k^2/k_\perp \propto k_\perp^{-5/3}$ is seen by satellites in the MHD range as the 1D Doppler frequency spectrum.

As the MHD and weakly dispersive KAW sub-ranges have very different slopes, the first spectral kink should appear at the wavenumber where their respective nonlinear interaction rates are equal. Comparing the nonlinear rates, $\gamma_k^{GS} = \gamma_{k\uparrow\downarrow}^{NL}$, we obtain the spectral kink wavenumber $\mu_1 \simeq 0.5$, at which the 1D spectrum should change from $-(3/2 \div 5/3)$ to $-(3 \div 4)$. The transition wavenumber for the $\gamma_k^{GS} = \gamma_{k\uparrow\uparrow}^{NL}$ transition is practically the same, $\mu_1 \simeq 0.6$.

However, above estimations did not take into account the weakening of MHD nonlinear interactions by the dynamic alignment between velocity and magnetic perturbations (Boldyrev, 2005) and/or by the nonlocal decorrelation mechanism proposed by Gogoberidze (2007). In general, the interaction rate can be written as a reduced GS rate (RGS)

$$\gamma_k^{RGS} \simeq R_{\lambda\perp} \gamma_k^{GS} \quad (21)$$

with the scale-dependent reducing coefficient $R_{k\perp}$. Both Boldyrev's and Gogoberidze's phenomenologies give the same scaling for $R_{k\perp}$,

$$R_{k\perp} \simeq \frac{v_{\lambda\perp}}{V_N} \propto \lambda_\perp^{1/4},$$

but with different normalization velocities V_N , such that the Boldyrev/Gogoberidze ratio $= v_L/V_A$, where v_L is the velocity amplitude at the driving scale L (wavenumber k_L). Having in mind that the dynamic alignment saturates when approaching small scales, the actual value of the Gogoberidze coefficient can be larger even in the case $v_L < V_A$. The reduced interaction rate proposed by Gogoberidze can be written as

$$\gamma_k^{RGS} \simeq R_{\lambda\perp} \left(\frac{v_{\lambda\perp}}{\lambda_\perp} \right) \simeq \left(\frac{k_\perp}{k_L} \right)^{-1/4} \left(\frac{1}{2\pi} k_\perp V_A \frac{B_k}{B_0} \right). \quad (22)$$

Given the typical width of the MHD inertial range in the solar wind $k_{b\perp}/k_L \sim 10^3$, we find that the interaction rate is reduced considerably in the vicinity of break points, $\gamma_k^{RGS} \simeq 0.25\gamma_k^{GS}$.

As the nonlocal decorrelation mechanism implies counter-propagating MHD waves, the counter-propagating KAWs

should undergo the same decorrelation. But co-propagating KAWs do not suffer from such decorrelation, and therefore we consider here the MHD/kinetic transition dominated by the nonlinear interaction among co-propagating KAWs. In addition, the co-propagating KAWs can keep in phase much longer than the counter-propagating KAWs. We therefore use (1) for kinetic and (21) for MHD interaction rate, and estimate the first spectral kink between the shallow MHD spectra $-(3/2 \div 5/3)$ and steep weakly dispersive KAW spectra $-(3 \div 5)$:

$$\mu_1 \simeq 0.6 \sqrt{R_{k\perp}}. \quad (23)$$

With Gogoberidze's rate (22) $\mu_1 \simeq 0.2$. But one should bear in mind that there are a number of factors, including a partial turbulence dissipation, which contribute to $R_{k\perp}$ and can make it smaller or larger than the Gogoberidze's value.

The second kink point should appear between weekly ($\mu_p^2 \ll 1$) and strongly ($\mu_p^2 \gg 1$) dispersive regimes of the KAW turbulence at

$$\mu_2 \gtrsim 1, \quad (24)$$

where we allow for a possible building-up of still steeper slope just above $\mu = 1$ in the cases where the MHD/KAW transition is not yet completed at $k_\perp = \rho_p^{-1}$. The spectrum slope above μ_2 , is $-(2.5 \div 3)$, which is significantly shallower than in the weakly dispersive range.

4.2 Spectral forms

The steepness of spectra in the weakly dispersive range depends on what kind of KAW turbulence picks up the turbulent cascade at $\mu \simeq 0.2$, weak or strong. If the critical balance condition holds at $\mu \simeq \mu_1$, then the turbulence of weakly dispersive KAWs is strong above μ_1 . In this case, strong KAW turbulence develops a steep energy spectrum $\propto k_\perp^{-3}$ in the weakly dispersive sub-range, connecting shallower MHD ($\propto k_\perp^{-5/3}$) and strongly dispersive KAW ($\propto k_\perp^{-7/3}$) spectra.

Significantly steeper spectra in both KAW sub-ranges can be produced by the weak KAW turbulence and by local deviations from the azimuthal symmetry of the turbulence (up to about $\propto k_\perp^{-4.5}$ in the weakly dispersive sub-range, and $\propto k_\perp^{-3}$ in the strongly dispersive sub-range). Transition to the weak turbulence regime may be facilitated by the partial wave dissipation via non-adiabatic ion acceleration/stochastic heating that does not depend on k_z but does depend on k_\perp reducing larger amplitudes at $k_\perp > k_{\perp\text{thr}}$. In such a way, the critical balance between linear and nonlinear time scales is violated in favor of weak turbulent regime. After that, the weak turbulent cascade of KAWs develops above $k_{\perp\text{thr}}$ and establishes steepest KAW spectra.

In both weak and strong turbulence regimes, the resulting spectra have two kinks, down and up, with the steepest slopes in between them in the weakly/mildly dispersive sub-range. In general, the "non-dissipative" scenario is as follows: the

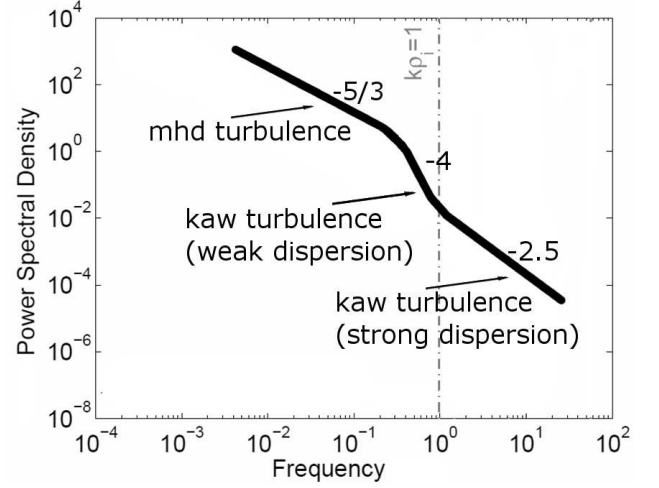


Fig. 2. Double-kink pattern produced by the MHD/weakly dispersive/strongly dispersive turbulence transitions. The kinetic KAW spectra are given for the weakly turbulent regime (in the strongly turbulent regime, spectra -4 and -2.5 are replaced by -3 and -7/3, respectively)

turbulence, driven at a large MHD scale L_{dr} ($k_{\text{dr}} = 2\pi/L_{\text{dr}}$), develop the shallowest $\propto k_\perp^{-3/2} \div k_\perp^{-5/3}$ spectra in the MHD sub-range $k_{\text{dr}} < k_\perp < k_{\perp 1}$, then it proceeds as a KAW turbulence with steepest $\propto k_\perp^{-3} \div k_\perp^{-4.5}$ spectra in the weakly dispersive sub-range $k_{\perp 1} < k_\perp \lesssim k_{\perp 2}$, and then above $k_{\perp 2}$ it proceeds as the KAW turbulence with $\propto k_\perp^{-7/3} \div k_\perp^{-3}$ spectrum in the strongly dispersive sub-range $k_{\perp 2} < k_\perp \lesssim k_{\perp\text{diss}}$. This last sub-range may extend to the dissipative wavenumber $k_{\perp\text{diss}}$ at electron length scale (Sahraoui et al., 2010).

Consequently, Alfvénic turbulent spectrum in the MHD/kinetic transition range attains an universal double-kink form (2-k pattern). This 2-k spectral pattern is shown schematically in Fig. 2 for the case of purely nonlinear non-dissipative transition. A (variable) slope of the weakly dispersive KAW spectrum depends on the ratio of turbulent energies cascading in strong and weak turbulent regimes, which can differ from case to case. The local slope should in principle lie between -3 and -4. But the shallower ζ -3 spectra can be produced by a fraction of the MHD cascade extending above the first kink, and the steeper ζ -4 spectra can be produced by azimuthal asymmetry of the turbulence in the cross-field plane.

A similar 2-k pattern can in principle be produced by the dissipative transition, suggested by many previous authors, but conditions required for that are rather special. Namely, the relative dissipation rate (as compared to the nonlinear interaction rate) should be much stronger in the range $k_{\perp 1} < k_\perp < k_{\perp 2}$ than in the range $k_\perp > k_{\perp 2}$.

In any case, the presence of a high-wavenumber cascade and turbulence at $k_\perp > k_{\perp 2}$ imply the nonlinear transfer and

spectral flux in the range $k_{\perp 1} < k_{\perp} \lesssim k_{\perp 2}$ as well, which means the nonlinear interaction should be taken into account. In real situations the relative importance of the effects due to dissipation versus weak turbulence versus strong turbulence in the MHD/kinetic turbulence transition can be different from case to case. The 2-k pattern described above can be noticed in many high-resolution high-frequency Cluster measurements (see examples in papers by Kyiani et al., 2009; Sahraoui et al., 2010; Chen et al., 2010), and can be also noticed in some previous measurements where frequency extended to 1 Hz or a little above (see e.g. Fig. 1 by Smith et al. 2006, showing ACE data).

An actual wavenumber range where super-adiabatic ion acceleration and related wave damping come into play is also variable. The threshold behavior suggests that with stronger spectral fluxes it comes into play earlier and weakens the MHD turbulence. In the cases where the flatness follows the trends shown in Fig. 3 by Alexandrova et al. (2008) for Cluster data, the super-adiabatic ion acceleration and partial wave damping may be active well below the apparent spectral kink.

5 Dissipation of KAWs

In this section we introduce several pros and cons concerning basic dissipations mechanisms for KAWs, but their detailed investigation is postponed for future.

Wu and Yang (2007) considered self-consistent velocities of minor ion species in KAW solitons and found them distributed proportionally to the ion mass-to-charge ratio. However, these velocities cannot be interpreted as thermal ones increasing temperature because they contribute to the non-thermal line broadening rather than thermal line width. A non-adiabatic disconnection from the wave fields is needed for the ions to gain some energy increase after the wave is passed by. Such process was considered by Voitenko and Goossens (2004), who shown that KAWs undergo strong non-adiabatic interaction with ions. This interaction require a certain threshold-like amplitude/wavelength relation for the dissipation switch-on, but does not require a long-time stochastic walk for the ions to gain a significant energy increase.

Chandran et al. (2010) have shown that another process related to non-adiabaticity - stochastic plasma heating - can absorb up to half of the turbulent cascade flux at $k_{\perp} \rho_p \sim 1$. This result implies the MHD nonlinear rate, which may be not true at $k_{\perp} \rho_p \sim 1$ where the KAW nonlinear interaction is faster and can pass more energy in the high- k_{\perp} range.

Yet another nonlinear interaction of the broadband Alfvénic turbulence with ions, via nonlinear Landau damping, was studied by Nariyuki et al. (2010), who shown that the ion heating proceeds both along and across the background magnetic field and produces asymmetric ion velocity distributions. On the other hand, because of the quasi-linear platea formation in velocity distribution functions, classic

Landau damping can be highly reduced in the weakly collisional solar wind (Voitenko and Goossens, 2006; Rudakov et al., 2011).

5.1 Landau damping

Parallel components of the KAW electric E_{zk} and magnetic B_{zk} fields make the KAWs efficient in Cherenkov interaction with plasma species via kinetic mechanisms of Landau and transit-time damping that were commonly used in estimations of KAW dissipation. However, these mechanisms are based on the resonant wave-particle interactions that depend strongly on the local parallel slopes of particle velocity distributions $F_s(V_z)$ at parallel velocities V_z equal to the wave phase velocity ω_k/k_z . In particular, quasi-linear diffusion reduces resonant slopes and Landau damping (Voitenko 2006):

$$\gamma_L = \sum_s \gamma_L^M \left(1 + \frac{\tau_C}{\tau_{KAW}} \right)^{-1}, \quad (25)$$

where γ_L^M is the Maxwellian Landau damping, and τ_{KAW} and τ_C are the characteristic diffusion times of particles due to KAWs and Coulomb collisions, respectively. KAWs flatten $F_s(V_z)$, Coulomb collisions restore it back to Maxwellian, and balance between two results in (25). Whereas the detailed analysis of (25) as function of k_{\perp} is quite complex (subject to separate study), our estimates, similar to that by Voitenko and Goossens (2006), show that for typical fluctuation level $W_f \sim 10^{-1}$ nT²/Hz at $k_{\perp} \rho_p \sim 1$ in the solar wind conditions $\tau_C/\tau_{KAW} \gg 1$ for both electrons and protons, and Landau damping is thus highly reduced. Therefore, conclusion by Podesta et al (2009) that the KAW turbulence cannot reach electron scales in the solar wind, based on the Maxwellian Landau damping, should by reconsidered.

5.2 Non-adiabatic threshold for turbulent dissipation

The rate of the non-adiabatic cross-field acceleration of the ions i by oblique Alfvén waves is (Voitenko and Goossens, 2004):

$$\gamma_{n-a}^2 = \Omega_i^2 \left[\frac{V_A}{\Omega_i} \left(\frac{c}{V_A} \frac{E_{\perp}}{B_{\perp}} - \frac{V_{iz}}{V_A} \right) \frac{\partial}{\partial x} \frac{B_{\perp}}{B_0} - 1 \right], \quad (26)$$

where V_{iz} is the parallel ion velocity, E_{\perp} and B_{\perp} are the Alfvénic electric and magnetic fluctuation, $\mathbf{E}_{\perp} \perp \mathbf{B}_{\perp}$.

Using $E_{\perp}/B_{\perp} \simeq V_A/c$ in the weakly dispersive range, and ignoring possible field-aligned streaming of ions, the threshold-like condition for this kind of wave-particle interaction, $\gamma_{n-a}^2 > 0$, can be written in the form

$$\eta_k = k_{\perp} \delta_p \frac{B_k}{B_0} > \nu_i, \quad (27)$$

where $\nu_i = \Omega_i/\Omega_p$ is the threshold value for η_k above which the particular ion species i is heated super-adiabatically.

The condition for ion acceleration apply for any particular ion specie, but the related wave dissipation depend on all ion species and their parameters, like species abundances, temperatures, etc. Nevertheless, condition for efficient wave dissipation can still be written in the form (27) with a super-adiabaticity η_k in the left hand side, but with different threshold ν_w in the right hand side, which is not easy to find. One can guess that the wave threshold should be close to the acceleration threshold for the dominant ion species $\nu_w \sim \nu_i$. Anyway, even without knowing the exact threshold value ν_w , it is possible to derive several useful scalings that can be tested observationally. So, for a power law scaling of magnetic amplitudes, $B_k^2 \propto k_\perp^{-q}$, we obtain the spectral dependence of the super-adiabaticity η_k :

$$\eta_k = \eta_{k1} \left(\frac{k_\perp}{k_{\perp 1}} \right)^{1-q/2}, \quad (28)$$

where B_{k1} is the reference magnetic amplitude at the reference length scale $\lambda_{\perp 1} = 2\pi/k_{\perp 1}$, and η_{k1} is the super-adiabaticity at $k_\perp = k_{\perp 1}$. For the sake of convenience we choose the reference wavenumber equal to wavenumber of the first spectral kink $k_{\perp 1}$.

Since $q \simeq 2/3$ in the MHD range, super-adiabaticity $\eta_k \propto k_\perp^{2/3}$ grows with k_\perp as long as $k_\perp < k_{\perp 1}$. But the situation is reversed in the weakly dispersive KAW range $k_\perp > k_{\perp 1}$, where $q \simeq 3$ and super-adiabaticity decreases with k_\perp as $\eta_k \propto k_\perp^{-1/2}$. Such spectral k_\perp -dependence of η_k indicates that the most favorable conditions for super-adiabatic ion heating and related wave dissipation are achieved in the vicinity of the first spectral kink, $k_\perp \simeq k_{\perp 1}$. This is shown schematically in Fig. 3, where we used the omnidirectional spectral representation $W_k \propto B_k^2/k_\perp \propto k_\perp^{-p}$ with $p = q + 1$. Since $p < 2$ ($\simeq 5/3$) in the MHD range, and $p > 3$ ($\simeq 4$) in the weakly dispersive KAW sub-range, the "threshold" spectrum

$$W_{\text{thr}} \propto \frac{B_{\text{thr}}^2}{k_\perp} \propto k_\perp^{-3}, \quad (29)$$

that follows from the super-adiabatic condition, can fall below the observed turbulent spectrum W_k around the first spectral kink.

Once the threshold $\eta_k = \nu_i$ is overcome in some wavenumber range for some ion species, the ions enter regime of strong acceleration. In turn, because of its threshold-like character, the super-adiabatic ion heating provides a highly selective dissipation mechanism for waves, affecting only strongest fluctuations with over-threshold amplitudes. In principle, the ability of turbulence to produce intermittent large-amplitude fluctuations increases the value of driven parameter (28), where one should use the spectrum and amplitudes of intermittent fluctuations instead of the regular turbulent spectrum. The eventual rate of the plasma heating and turbulence dissipation should follow from the balance between two processes: (i) production of the over-threshold intermittent fluctuations by the turbulence, and (ii)

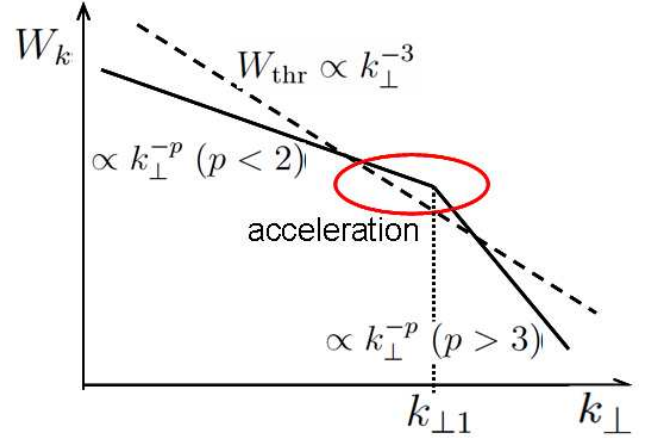


Fig. 3. Typical Alfvénic turbulent spectrum (solid line) in the weakly/mildly dispersive KAW sub-range and "threshold" turbulent spectrum (dashed line) required for the super-adiabatic ion acceleration. Super-adiabatic acceleration is possible around the first spectral kink, where the turbulent spectral power raises above the threshold spectral power.

accommodation of turbulence energy by accelerated ions and its further redistribution into the bulk plasma. Helios observations have shown that the flatness (measure of intermittency) increases with increasing wavenumber (Alexandrova et al., 2008), which progressively increases the super-adiabaticity parameter above the value given by (28). Then, at some large enough wavenumber, the level of intermittent fluctuations can reach the super-adiabatic threshold even if the regular turbulent level remain below it. .

Dissipation due to super-adiabatic heating/acceleration tends to reduce the over-threshold fluctuations at every scale to the corresponding threshold value given by (27). Then, in accordance to (27), the upper bound for the reduced intermittent amplitudes scales as $B_{\text{thr}}^2 \propto k_\perp^{-2}$, and since the magnetic power spectrum in this range has shallower scaling $B_k^2 \propto k_\perp^{-2/3}$, the flatness (and higher order normalized structure functions as well) should decrease with wavenumber in the MHD range below the first spectral kink. This can explain another interesting feature, a local decrease of the flatness in the spacecraft frequency range $0.02 \div 0.2$ Hz (which is still below the apparent spectral kink), found by Alexandrova et al. (2008) using Cluster data. We suggest that such behavior of the flatness may indicate a partial dissipation of Alfvén waves via super-adiabatic ion acceleration in the corresponding wavenumber range.

In turn, highly anisotropic ion distributions are produced by super-adiabatic acceleration (Voitenko and Goossens, 2004), which can drive anisotropic ion-cyclotron instabilities redistributing energy further. Since the super-adiabatic ion acceleration is very fast, within a fraction of the corresponding ion gyroperiod, the quasi-stationary rate of tur-

bulent dissipation will be determined by the ion-cyclotron instability increment. The situation is thus more complex here and opposite to that observed in hydrodynamics, where viscosity washes out smallest amplitudes when approaching the dissipation range, but large-amplitude fluctuations survive increasing intermittency. The behavior of the intermittency found by Alexandrova et al. (2008) is not typical for the linear Landau damping as well.

After the relative perpendicular/parallel power in the spectrum and the strength of MHD interaction are reduced, the transition to the weak KAW turbulence is made possible and leads to the steepest spectra in the weakly dispersive sub-range. It would be interesting to analyze intermittency by the Rank-Ordered Multifractal Analysis (ROMA) (see Chang et al., 2010, and references therein), which would allow to find out if the solar wind turbulence possesses different fractal properties in the three mentioned above sub-ranges.

6 Summary and Discussion

For the first time, a weakly dispersive sub-range of the KAW turbulence is distinguished and studied in the context of MHD/kinetic turbulence transition. We show that the KAW turbulence and its spectra in the weakly dispersive sub-range differ significantly not only from the conventional MHD Alfvénic turbulence, but also from the strongly dispersive KAW turbulence. Namely, the nonlinear interaction of weakly dispersive KAWs is capable to produce steepest spectra $\propto k_{\perp}^{-3} \div k_{\perp}^{-5}$ in the wavenumber range $k_{\perp 1} < k_{\perp} < \rho_p^{-1}$, connecting shallow MHD spectra $\propto k_{\perp}^{-3/2} \div k_{\perp}^{-5/3}$ below the first spectral kink, $k_{\perp} < k_{\perp 1}$, and "intermediate" $\propto k_{\perp}^{-7/3} \div k_{\perp}^{-3}$ spectra of strongly dispersive KAWs above the second spectral kink, $k_{\perp} > \rho_p^{-1}$.

The universal spectral form - 2-k pattern resulting from such spectral dynamics in the transition range is shown schematically in Fig. 2. Turbulent spectra observed recently by the Cluster spacecraft often exhibit such 2-k pattern in the transition wavenumber range (see for example Fig.1). It is still not certain what is the role of Landau damping in producing so steep spectral drop at $k_{\perp} \rho_p \lesssim 1$. Any kind of kinetic dissipation in the weakly collisional solar wind should be self-consistently saturated at a reduced level by the local plateau formation in the velocity distribution functions of plasma species. At least a quasi-linear theory is needed to account for the particles' feedback reaction on the energy input from the waves, and numerous previous estimations based on the Maxwellian Landau damping should be re-evaluated.

Podesta (2009) reported a significant flattening of the high-frequency parallel spectra and suggested it may be due to a plasma instability injecting a fraction of parallel propagating waves. On the other hand, this flattening can be produced by the transition to the weak KAW turbulence, possessing (in an ideal case) a very shallow spectrum (10). However, because of many interfering factors, it is not certain if the parallel

wavenumber spectrum (10) can be realized in the solar wind. The perpendicular wavenumber spectra are determined by the nonlinear interaction among perpendicular length scales and are thus quite robust. But the corresponding parallel wavenumber dynamics and spectra follow the perpendicular wavenumber dynamics and are often defined from a suitable functional form linking them to the perpendicular ones. This functional form may depend on a number of factors, including strength of the turbulence, partial turbulence dissipation, etc. In the extreme cases of weak and strong turbulence, the parallel dynamics is fixed, respectively, by the perpendicular one kinematically (via resonant conditions) and by adjusting linear and nonlinear time scales (via critical balance condition).

One can expect a high variability of spectral slopes in the weakly dispersive wavenumber sub-range, resulting from a mixture of several "pure" spectra that can be produced by KAWs in this range. In addition, our analysis suggests the super-adiabatic and/or stochastic cross-field acceleration of the solar wind ions as feasible mechanisms for a partial KAWs dissipation operating in the vicinity of first spectral kink. Both these mechanisms share the same non-adiabatic threshold and imply a *selective dissipation* of the over-threshold fluctuations with largest amplitudes. This kind of dissipation reduces high-amplitude intermittent fluctuations and should therefore produce local decrease of flatness in the dissipation range. Albeit there are observational indications for such behavior of flatness (see Fig. 3 by Alexandrova et al., 2008), this point needs further observational support.

It seems that the synergetic action of selective wave dissipation and weak turbulence of KAWs influences both the spectral kink positions and the spectral slopes, making them dependent of the turbulence level. Namely, η_k , product of the turbulent amplitude and corresponding wavenumber, is the parameter facilitating transition to the weak KAW turbulence with its steeper spectra. As the spectral flux $\sim \eta_k^3$, the larger spectral fluxes imply larger η_k , which in turn imply steeper spectra in the weakly dissipative range. Such a counter-intuitive trend was found by Smith et al. (2006).

On the other hand, in the vicinity of spectral kinks the non-adiabatic wave-particle interaction tends to reduce η_k to a near-threshold value, which results in the scaling $B_{k1} \sim k_{\perp 1}^{-1}$. This scaling offer an explanation for observed spectral kink wavenumbers that were found to be inversely proportional to the fluctuation amplitudes at spectral kinks (Markovskii et al., 2008).

Contrary to MHD Alfvén waves, the dispersion law of KAWs, even weakly dispersive, is not degenerated with respect to k_{\perp} . This makes possible 3-wave interactions with all 3 waves residing on the KAW branch, and there is no need in a zero- k_{\parallel} , $k_{\perp} \neq 0$ mode mediating the MHD turbulent cascade. Consequently, an additional spectrum of the KAW turbulence can be created by the cascading enstrophy (dispersive part of energy). The energy and the enstrophy cascade in opposite directions from the injection wavenum-

ber. As the turbulence of KAWs in the solar wind is driven at largest near-MHD length scales, it naturally proceed to smaller scales following a direct cascade route. In other circumstances, and with different positions of the driving scale, one may observe inverse (e.g. Lui et al., 2008), or dual spectral transport, which is not easy to discriminate and describe in terms of cascades because of the non-local contaminations and scale mixing in a real finite-size and high-variable environment (see Vörös et al., 2010).

Again, contrary to the MHD AW turbulence, the KAW turbulence does not require the pre-existing counter-propagating waves for efficient cascading. Nonlinear interaction among co-propagating KAWs is strong enough to establish a co-propagating (completely imbalanced) KAW turbulence without involving the counter-propagating KAWs. If the co-propagating KAW turbulence develops in some wavenumber range (e.g. at $k_{\perp 1} < k_{\perp} < \rho_p^{-1}$), then the ratio of sunward/anti-sunward Poynting fluxes should be frozen and remain approximately constant at these wavenumbers. This would provide another observational benchmark for the KAW turbulence, but we are not aware about such observations so far.

Acknowledgements. This work was supported in part by STCE (Solar-Terrestrial Center of Excellence) under the project "Fundamental science". Some results of this paper were presented and discussed at the Turbulence and Multifractals Workshop (8-11 June 2010, Brussels, Belgium).

References

- Alexandrova, O., Carbone, V., Veltri, P., and L. Sorriso-Valvo: Small-scale energy cascade of the solar wind turbulence, *Astrophys. J.*, 674, 1153–1157, doi:10.1086/524056, 2008.
- Bale, S. D., P. J. Kellogg, F. S. Mozer, T. S. Horbury, and H. Reme: Measurement of the electric fluctuation spectrum of magnetohydrodynamic turbulence, *Phys. Rev. Lett.*, 94(21), 215002, doi:10.1103/PhysRevLett.94.215002, 2005.
- Boldyrev, S.: On the Spectrum of Magnetohydrodynamic Turbulence, *Astrophys. J.*, 626, L37–L40, 2005.
- Carbone, V.; Perri, S.; Yordanova, E.; Veltri, P.; Bruno, R.; Khotyaintsev, Y.; André, M.: Sign-Singularity of the Reduced Magnetic Helicity in the Solar Wind Plasma, *Phys. Rev. Lett.*, 104, id. 181101, 2010.
- Chandran, Benjamin D. G.; Li, Bo; Rogers, Barrett N.; Quataert, Eliot; Germaschewski, Kai: Perpendicular Ion Heating by Low-frequency Alfvén-wave Turbulence in the Solar Wind, *Astrophys. J.*, 720, 503–515, 2010.
- Chang, T.; Wu, C. C.; Podesta, J.; Echim, M.; Lamy, H.; Tam, S. W. Y.: ROMA (Rank-Ordered Multifractal Analyses) of intermittency in space plasmas – a brief tutorial review, *Nonl. Proc. Geophys.*, 17, 545–551, 2010.
- Chen, C. H. K.; Horbury, T. S.; Schekochihin, A. A.; Wicks, R. T.; Alexandrova, O.; Mitchell, J.: Anisotropy of Solar Wind Turbulence between Ion and Electron Scales, *Phys. Rev. Lett.*, 104, id. 255002, 2010.
- Gogoberidze, G.: On the nature of incompressible magnetohydrodynamic turbulence, *Phys. Plasmas*, 14, pp. 022304–022304–11, 2007.
- Hasegawa, A. and Chen, L.: Kinetic processes in plasma heating by resonant mode conversion of Alfvén wave, *Phys. Fluids*, 19 (12), 1924–1934, 1976.
- Howes, G. G., Cowley, S. C., Dorland, W., Hammett, G. W., Quataert, E., and Schekochihin, A. A.: A model of turbulence in magnetized plasmas: Implications for the dissipation range in the solar wind, *J. Geophys. Res.*, 113, 5103, doi:10.1029/2007JA012665, 2008.
- Kiyani, K. H.; Chapman, S. C.; Khotyaintsev, Yu. V.; Dunlop, M. W.; Sahraoui, F.: Global Scale-Invariant Dissipation in Collisionless Plasma Turbulence, *Phys. Rev. Lett.*, 103, id. 075006, 2009.
- Leamon, R. J., Smith, C. W., Ness, N. F., and Wong, H. K.: Dissipation range dynamics: Kinetic Alfvén waves and the importance of electron β_e , *J. Geophys. Res.*, 104, 22 331–22 344, doi:10.1029/1999JA900158, 1999.
- Lui, A. T. Y.; Yoon, P. H.; Mok, Chinook; Ryu, Chang-Mo: Inverse cascade feature in current disruption, *J. Geophys. Res.*, 113, Issue 6, CiteID A00C06, 2008.
- Markovskii, S. A., Vasquez, B. J., and Smith, C. W.: Statistical analysis of the high-frequency spectral break of the solar wind turbulence at 1 AU, *Astrophys. J.*, 675, 1576–1583, 2008.
- Nariyuki, Y.; Hada, T.; Tsubouchi, K.: Heating and acceleration of ions in nonresonant Alfvénic turbulence, *Phys. Plasmas*, 17, 072301–072301–5, 2010.
- Podesta, J. J. Dependence of Solar-Wind Power Spectra on the Direction of the Local Mean Magnetic Field, *Astrophys. J.*, 698, 986–999, 2009.
- Podesta, J. J.; Borovsky, J. E.; Gary, S. P.: A Kinetic Alfvén Wave Cascade Subject to Collisionless Damping Cannot Reach Electron Scales in the Solar Wind at 1 AU, *Astrophys. J.*, 712, 685–691, 2010.
- Rudakov, L.; Mithaiwala, M.; Ganguli, G.; Crabtree, C.: Linear and nonlinear Landau resonance of kinetic Alfvén waves: Consequences for electron distribution and wave spectrum in the solar wind, *Phys. Plasmas*, 18, 012307–012307–10, 2011.
- Sahraoui, F.; Goldstein, M. L.; Belmont, G.; Canu, P.; Rezeau, L.: Three Dimensional Anisotropic k Spectra of Turbulence at Subproton Scales in the Solar Wind, *Phys. Rev. Lett.*, 105, id. 131101, 2010.
- Schekochihin, A. A., Cowley, S. C., Dorland, W., Hammett, G. W., Howes, G. G., Quataert, E., and Tatsuno, T.: Astrophysical gyrokinetics: Kinetic and fluid turbulent cascades in magnetized weakly collisional plasmas, *Astrophys. J. Suppl.*, 182, 310–377, doi:10.1088/0067-0049/182/1/310}, 2009.
- Smith, C. W., Hamilton, K., Vasquez, B. J., and Leamon, R. J.: Dependence of the Dissipation Range Spectrum of Interplanetary Magnetic Fluctuations on the Rate of Energy Cascade, *The Astrophysical Journal Letters*, 645, L85–L88, doi:10.1086/506151, 2006.
- Voitenko, Yu. M.: Three-wave coupling and parametric decay of kinetic Alfvén waves, *J. Plasma Phys.* 60, 497, 1998a.
- Voitenko, Yu. M.: Three-wave coupling and weak turbulence of kinetic Alfvén waves, *J. Plasma Phys.* 60, 515, 1998b.
- Voitenko, Y. and M. Goossens: Cross-Field Heating of Coronal Ions by Low-Frequency Kinetic Alfvén Waves, *Astrophys. J.* 605, L149–L152, doi:10.1086/420927, 2004.

- Voitenko, Y. and M. Goossens: Energization of Plasma Species by Intermittent Kinetic Alfvén Waves, *Space Sci. Rev.*, 122, 255-270, 2006.
- Vörös, Z.; Runov, A.; Leubner, M. P.; Baumjohann, W.; Volwerk, M.: Is current disruption associated with an inverse cascade? *Nonl. Proc. Geophys.*, 17, pp.287-292, 2010
- Luo, Q. Y.; Wu, D. J.: Observations of Anisotropic Scaling of Solar Wind Turbulence, *Astrophys. J.*, 714, L138-L141, 2010.
- Wu, D. J.; Yang, L. Nonlinear Interaction of Minor Heavy Ions with Kinetic Alfvén Waves and Their Anisotropic Energization in Coronal Holes, *Astrophys. J.*, 659, Issue 2, pp. 1693-1701, 2007.